# 320 Gb/s Unamplified Transmission using 100 GHz Ge PD and TFLN MZM on a Foundry-Compatible SiPh Platform Co-Packaged with Traveling-Wave Drivers and TIAs

Jakob Declercq(1), Shengpu Niu(1), Margot Niels(2), Amir Shahin(2,3), Joris Van Kerrebrouck(1),
Maximilien Billet(2), Mathias Berciano(3,†), Joris Lambrecht(1,†), Bart Moeneclaey(1), Tom Vanackere(2),
Ewoud Vissers(2), Conor Coughlan(3), Gunther Roelkens(2), Arno Moerman(1), Olivier Caytan(1),
Sam Lemey(1), Maumita Chakrabarti(3), Hakim Kobbi(3), Minkyu Kim(3), Didit Yudistra(3), Roger Loo(3,4),
Swetanshu Bipul(3), Filippo Ferraro(3), Yoojin Ban(3), Peter De Heyn(3), Guy Torfs(1), Johan Bauwelinck(1),
Dimitrios Velenis(3), Peter Ossieur(1), Philippe Absil(3), Bart Kuyken(2), Joris Van Campenhout(3),
Nishant Singh(1), Cedric Bruynsteen(1), Xin Yin(1)

(1) IDLab, INTEC, imec-Ghent University, 9052 Ghent, Belgium, cedric.bruynsteen@imec.be
(2) Photonics Research Group, INTEC, imec-Ghent University, 9052 Ghent, Belgium,
(3) imec, 3001 Leuven, Belgium,
(4) Department of Solid-State Sciences, Ghent University, 9000 Ghent, Belgium,
(†) No longer affiliated

***Abstract*** *We demonstrate a 2 km 160 GBd PAM-4 O-band link with traveling-wave drivers and TIAs co-packaged with a new high-responsivity 100 GHz Ge photodetector and transfer printed TFLN MZMs on a silicon photonics platform. ©2025 The Author(s)*

## Introduction

The explosive growth in data demand, accelerated by AI adoption, has created stringent requirements for data center interconnects. Current short-range links predominantly employ intensity modulation/direct detection (IM/DD) in the O-band, with 200 Gb/s per lane as the present standard, while next-generation specifications target 400 Gb/s per lane[1]. Achieving these targets necessitates both novel mass-producible optical devices and advanced electronic circuits with optimized assembly techniques to deliver cost-effective, high-performance links.

Silicon photonics (SiPh) platforms present an attractive solution for mass-produced, low-cost photonic integrated circuits due to their large wafer sizes and existing tooling capacity. However, current generation SiPh platforms are constrained by the bandwidth limitations of existing electro-optical-electrical (EOE) components, particularly photodetectors (PDs) and modulators. Silicon carrier depletion-based Mach-Zehnder modulators (MZMs) have not yet achieved sufficient bandwidth, while germanium photodetectors have demonstrated high bandwidth capabilities however with low responsivity and difficult integration challenges due to complex manufacturing processes[2]. A significant market opportunity exists for high-speed modulators and photodiodes that can be manufactured efficiently using existing CMOS fabrication infrastructure on a monolithic platform. Wafer-scale heterogeneous integration can extend the capability of silicon photonics by incorporating high-speed thin-film lithium niobate (TFLN) devices and III-V lasers. Thanks to the back-end integration approach, transfer printing maintains compatibility with standard CMOS processing while enabling the incorporation of advanced materials. In addition to high-speed optical devices, high-speed linear electronics are essential to maximize signal integrity and enable higher modulation orders such as PAM-4.

In this paper, we demonstrate an O-band 320 Gb/s unamplified optical link over 2 km of standard single-mode fiber (SSMF) using novel high-bandwidth integrated circuits. The transmitter incorporates a four-channel fully differential traveling-wave driver connected to a four-channel differential hybrid TFLN MZM, implemented through transfer printing on imec's 200 mm SiPh platform. At the receiver, we employ a 100 GHz silicon-contacted germanium photodiode monolithically integrated on imec's 300 mm SiPh platform, connected to a four-channel traveling-wave transimpedance amplifier (TIA). This experimental demonstration highlights the potential of a transfer-printing-enhanced SiPh platform to meet the requirements for next-generation 400 Gb/s per lane IM/DD transceivers.

## Enhanced SiPh platform devices

Figure 1(a) shows a simplified cross-section of the envisioned SiPh platform put forward in this work. The platform combines the typical key components, including Si waveguides with dopants, heaters for efficient low-speed thermal tuning, a silicon nitride (SiN) layer for low-loss propagation

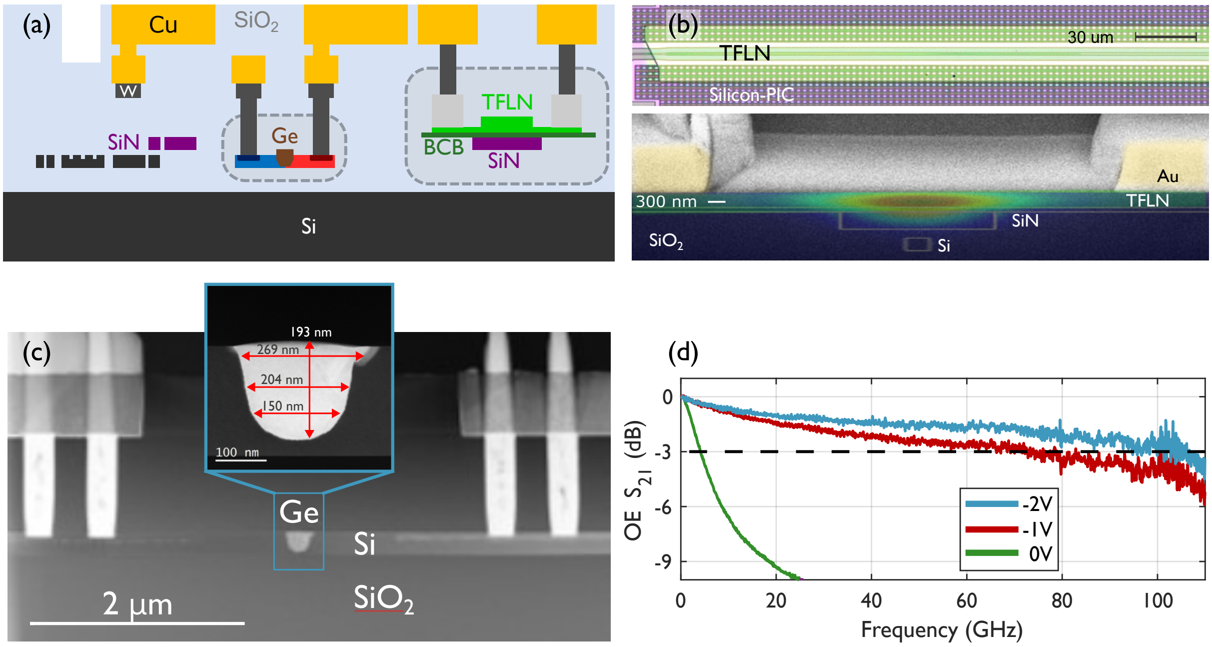

**Fig. 1:** (a) Simplified overview of the envisioned next-generation SiPh platform. (b) Image after the integration of TFLN on a Si-PIC and SEM of a FIB cross-section of the heterogeneous EO device on a Si-PIC. (c) TEM images of the Ge/Si PD, showing the Ge growth in the deeply recessed Si cavity (d) Measured optoelectronic bandwidth of the Ge photodiode.

and high-quality filtering, and germanium photodetectors. The platform is enhanced by the addition of transfer printed TFLN modulators[3]. State-of-the-art TFLN modulators have been demonstrated to reach a BW of 100 GHz[4].

The 7 mm long modulator consists of a SiN Mach-Zehnder interferometer from a commercial SiPh platform, where TFLN is heterogeneously integrated on both arms through transfer printing[3]. The device architecture is designed in a push-pull configuration, achieved by the rotation of the TFLN crystal orientation in each modulator arm. The electro-optic modulation occurs in the resulting hybrid SiN/LN optical mode, driven by Ti/Au electrodes. A top view of a hybrid SiN/LN waveguide modulator arm is depicted in Figure 1(b), followed by a scanning electron microscope (SEM) image of a cross-section of the heterogeneous electro-optic platform. The aforementioned modulator typically shows a low half-wave voltage ($V_\pi$) of 4 V and an extinction ratio of 32 dB for a wavelength of 1310 nm. The MZM chip exhibits an end-to-end insertion loss of 16.2 dB, comprising 5.1 dB from the MZM itself and 11.1 dB from waveguide routing and grating couplers. Future designs could substantially reduce losses by implementing low-loss SiN waveguides for routing and incorporating high-efficiency grating or edge couplers.

The photodiode shown in the transmission electron microscopy (TEM) image in Figure 1(c) is fabricated in imec's 300 mm silicon photonics platform[5], based on 220 nm silicon on insulator (SOI) wafers with a buried oxide layer depth of 2 µm. Following ion implantation of N and P dopants and subsequent annealing, the Si is etched to form a deeply recessed cavity into which Ge is grown to the top Si surface via selective epitaxy. The resulting Ge absorption region has very small cross-sectional dimensions (about 200 nm high and 150-270 nm wide) and is deeply embedded into the doped Si layer. Therefore, a high electric field is created in the Ge absorption layer upon reverse biasing the Si p-i-n diode, allowing the photogenerated carriers to travel at their saturation velocity and minimizing their transit time out of the narrow absorption region. The compact nature of the photodiode allows it to achieve very low junction capacitance (<5 fF) which, together with the low transit time, results in a high analog bandwidth of 100 GHz into a 50 $\Omega$ load (Fig. 1(d)). The photodiode combines high-frequency performance with a high responsivity of 0.9 A/W at 1 V reverse bias, measured at a wavelength of 1310 nm.

## Assembly and Transmission Experiments

The electronic chips used in this transceiver are multi-stage traveling wave drivers and TIAs designed in a 55 nm SiGe BiCMOS technology with a nominal $f_T$ of 320 GHz. The TIA has a single-ended input and a differential output with a maximum transimpedance gain of 77 dB$\Omega$[6]. The driver has a differential input and output with a gain range of 11.2 dB to 21.8 dB at an output swing of 3.4 Vppd[7]. Both electronic chips have SPI interfaces, which provide control over gain and level of peaking.

The photonic chips were diced and assembled with the electronic chips on PCBs using wirebonds. Extra care was taken to ensure the dicing street was close to the high-speed pads to minimize wirebond inductance. The submounts of the PCBs

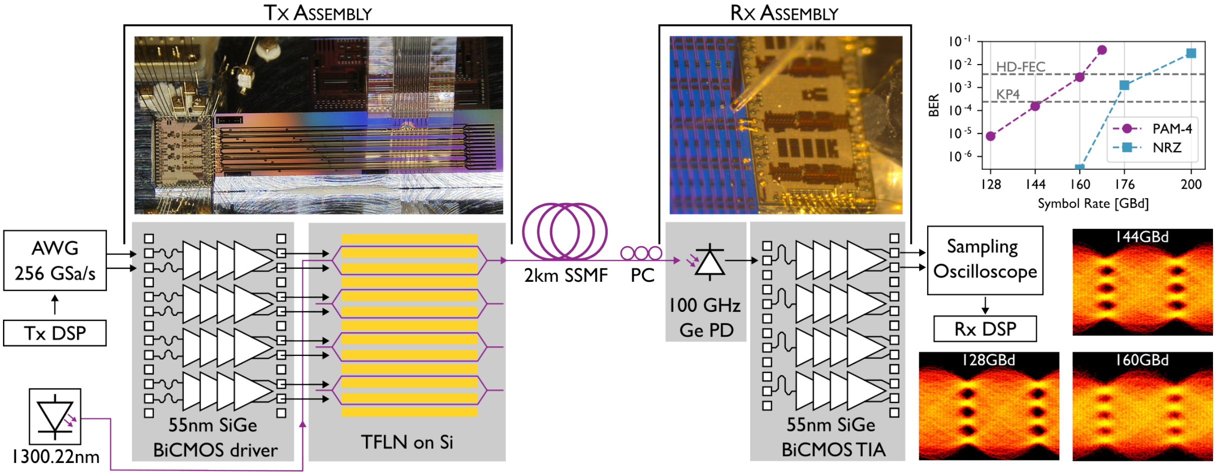

**Fig. 2:** Experimental setup for transmission measurements showing transmit and receive assemblies along with eye diagrams and BER curves.

were milled to compensate for the height difference between the ICs. Furthermore, wedge-wedge bonds were used to make sure the loop height was minimal. A fiber array was attached to the transmit side assembly using UV-curable epoxy, while a single fiber was used for the receive side assembly.

The O-band link was established as shown in Figure 2 using a Keysight M8199B 256 GS/s AWG as the signal source and a Keysight DCA-X 100 GHz sampling oscilloscope at the receiver. The asymmetric TFLN MZM is biased to its quadrature position by setting the wavelength to 1300.22 nm. To compensate for part of the losses in the MZM chip, an additional booster amplifier was placed after the laser, mimicking a single high-power laser. The PRBS-15 signal generated by the AWG was fed into the driver input of the transmitter assembly and transmitted over 2 km of SSMF to the receiver assembly. The optical signal, with an average power of 2.5 dBm after the modulator at quadrature bias, was received without any optical amplification or optical filtering techniques. The frequency response of the entire link was characterized and compensated at the AWG using Keysight's IQTools software.

A fractionally spaced 32-tap FFE combined with an 8-tap DFE was applied on the oscilloscope to process the received signal, enabling the capture of NRZ and PAM-4 eye diagrams. By counting the errors in the received signal with respect to the transmitted signal, the BER was determined. As shown in the rightmost part of Figure 2, NRZ remains error-free up to 160 GBd. At 144 GBd, the PAM-4 signal achieved a BER of 1.53E-4, remaining below the KP-4 FEC threshold, while at 160 GBd, it reached a BER of 2.8E-3, staying within the 6.7% HD-FEC limit. Operating at a gross data rate of 320 Gb/s, the link demonstrated a power efficiency of 4 pJ/bit, excluding the laser and DSP power consumption.

## Conclusions

In this work we demonstrated a 2 km PAM-4 modulated O-band link without optical amplification operating at a gross data rate up to 320 Gb/s, achieving a BER below the 6.7% HD-FEC threshold. Our implementation leverages novel high-speed integrated circuits fully compatible with standard CMOS fabrication processes. These include custom-designed traveling-wave drivers and TIAs, a high-bandwidth Ge photodiode and transfer-printing enabled TFLN modulators on Si, representing a significant advancement in hybrid photonic integration. We believe that these results show the strong potential of deploying hybridized SiPh for cost-effective next-generation 400 Gb/s per lane links.

## Acknowledgements

This work is partially supported by imec's industrial affiliation R&D program on Optical I/O, imec's AAA program, imec invest R&D project LNO-EIC co-design, FWO and Ghent University Special Research Fund 01G02720. The authors would like to thank the platform, devices and assembly teams.

## References

[1] P. A. Baziana, "Optical Data Center Networking: A Comprehensive Review on Traffic, Switching, Bandwidth Allocation, and Challenges", *IEEE Access*, vol. 12, pp. 186 413–186 444, 2024. DOI: `10.1109/ACCESS.2024.3513214`.

[2] S. Lischke, A. Peczek, J. Morgan, K. Sun, D. Steckler, Y. Yamamoto, F. Korndörfer, C. Mai, S. Marschmeyer, M. Fraschke, A. Krüger, A. Beling, and L. Zimmermann, "Ultra-fast germanium photodiode with 3-dB bandwidth of 265 GHz", *Nature Photonics*, vol. 15, Mar. 2021. DOI: `10.1038/s41566-021-00948-y`.

[3] M. Niels, T. Vanackere, T. Vandekerckhove, S. Poelman, T. Reep, G. Roelkens, M. Billet, and B. Kuyken, "Centimetre-scale micro-transfer printing to enable heterogeneous integration of thin film lithium niobate with silicon photonics", *Optical Materials Express*, vol. 15, no. 3, pp. 531–540, Mar. 2025. DOI: `10.1364/OME.551748`.

[4] C. Wang, M. Zhang, M. Bertrand, A. Shams-Ansari, S. Chandrasekhar, P. Winzer, and M. Loncar, “Integrated lithium niobate electro-optic modulators operating at CMOS-compatible voltages”, *Nature*, vol. 562, Oct. 2018. DOI: `10.1038/s41586-018-0551-y`.

[5] F. J. Ferraro, P. D. Heyn, M. Kim, N. Rajasekaran, M. Berciano, G. Muliuk, D. Bode, G. Lepage, S. Janssen, R. Magdziak, J. D. Coster, H. Kobbi, S. Lardenois, N. Golshani, L. Shiramin, C. Marchese, S. Rajmohan, S. Nadarajan, N. Singh, S. Radhakrishnan, A. Tsiara, P. Xu, A. Karagoz, D. Yudistira, M. Martire, A. Shahar, M. Chakrabarti, D. Velenis, W. Guo, A. Miller, K. Croes, S. Balakrishnan, P. Verheyen, Y. Ban, J. V. Campenhout, and P. P. Absil, “imec silicon photonics platforms: performance overview and roadmap”, in *SPIE OPTO*, vol. 12429, SPIE, 2023, p. 1 242 909. DOI: `10.1117/12.2650579`.

[6] J. Declercq, B. Moeneclaey, J. Lambrecht, C. Bruynsteen, N. Singh, S. Niu, P. Ossieur, and X. Yin, “A 64-GHz Optical Receiver for 128-GBd Links Using a 55-Nm SiGe BiCMOS Traveling-Wave Linear Transimpedance Amplifier”, *Journal of Lightwave Technology*, vol. 43, no. 9, pp. 4139–4148, 2025. DOI: `10.1109/JLT.2025.3533200`.

[7] S. Niu, R. Ahmed, J. Lambrecht, J. Declercq, M. Verbeke, M. Verplaetse, B. Moeneclaey, C. Wang, J. V. Kerrebrouck, N. Singh, J. Bauwelinck, and X. Yin, “A Linear Modulator Driver With Over 70-GHz Bandwidth 21.8-dB Gain and 3.4-Vppd Output Swing for Beyond 120-GBd Optical Links”, *IEEE Transactions on Microwave Theory and Techniques*, vol. 72, no. 7, pp. 4080–4091, 2024. DOI: `10.1109/TMTT.2023.3342624`.